Technical Paper by J.D. Bray and S.M. Merry

A Comparison of the Response of Geosynthetics in the Multi-Axial and Uniaxial Test Devices

ABSTRACT: The wide strip tension test imposes boundary conditions that vary from a uniaxial stress state near the middle of the specimen to a plane-strain, biaxial stress state at the clamps. The multi-axial tension test imposes boundary conditions that vary from a plane-strain, biaxial stress state at the restraining ring to a nearly isotropic, biaxial stress state at the center. To evaluate the influence of the stress state induced during testing on the stress-strain response of geomembranes, strain-controlled multi-axial and wide strip tests were performed on specimens of elastic latex, polyvinyl chloride (PVC), and high density polyethylene (HDPE). The ratio of the secant Young's modulus in the multi-axial test to that in the wide strip uniaxial test was approximately 1.2 for the nearly linear, elastic latex membrane, which is substantially less than the theoretically derived value of 2.0. This ratio was approximately 1.4 and 1.9 for PVC and HDPE geomembranes at 1% strain, respectively, indicating greater differences between measured multi-axial and uniaxial responses with materials exhibiting more nonlinearity. Strength values measured in the tests were similar, but the uniaxial test overestimated the ductility (i.e. failure strain) of the HDPE geomembrane. Wider use of the multi-axial test device is recommended for cases where the geomembrane deforms in a biaxial stress state, and material ductility and stiffness are important.

KEYWORDS: Failure, Geomembrane, Geosynthetic, Multi-Axial tension test, Stress-strain, Uniaxial tension test, Wide strip tension test.

AUTHORS: J.D. Bray, Associate Professor, Department of Civil and Environmental Engineering, University of California, Berkeley, California 94720-1710, USA, Telephone: 1/510-642-9843, Telefax: 1/510-642-7476, E-mail: bray@ce.berkeley.edu; and S.M. Merry, Assistant Professor, Department of Civil and Environmental Engineering, University of Utah, Salt Lake City, Utah 84112-0561, USA, Telephone: 1/801-585-9726, Telefax: 1/801-585-5477, E-mail: merry@civil.utah.edu.

PUBLICATION: *Geosynthetics International* is published by the Industrial Fabrics Association International, 1801 County Road B West, Roseville, Minnesota 55113-4061, USA, Telephone: 1/651-222-2508, Telefax: 1/651-631-9334. *Geosynthetics International* is registered under ISSN 1072-6349.

DATES: Original manuscript received 31 July 1998, revised version received 23 December 1998 and accepted 24 December 1998. Discussion open until 1 September 1999.

REFERENCE: Bray, J.D. and Merry, S.M., 1999, "A Comparison of the Response of Geosynthetics in the Multi-Axial and Uniaxial Test Devices", *Geosynthetics International*, Vol. 6, No. 1, pp. 19-40.

1 INTRODUCTION

Evaluation of the mechanical response of geosynthetics through controlled laboratory testing is integral to designing systems involving geosynthetics (e.g. containment systems, mechanically stabilized earth walls, and reinforced structural fill overlying soft ground). Due to its visco-elastoplastic response, the characterization of the geosynthetic's mechanical response often includes measurement of its stress-strain-time response at a specified temperature under the likely chemical environment. The laboratory test device utilized to measure the geosynthetic's mechanical response should optimally maintain boundary conditions that induce stress and strain fields that are representative of the field loading conditions. However, this optimal situation may not be achievable while maintaining the simplicity of the test boundary conditions that allow the acquired data to be interpreted unambiguously. Consequently, standardization of the test device, procedure, and interpretation is typically achieved, and the design engineer is often left with the difficult task of relating measured geosynthetic response in the laboratory with its anticipated performance in the field under different loading conditions.

In the current paper, two performance tests standardized by the American Society for Testing and Materials (ASTM) that are available to evaluate the stress-strain response of geomembranes are examined and compared. These tests are commonly referred to as the multi-axial tension test (ASTM D 5617 *Standard Test Method for Multi-Axial Tension Test for Geosynthetics*) and the wide strip tension test (ASTM D 4885 *Standard Test Method for Determining Performance Strength of Geomembranes by the Wide Strip Tensile Method*). Test methods for assessing the tensile characteristics of plastics (ASTM D 638 *Standard Test Method for Tensile Properties of Plastics*; and ASTM D 882 *Standard Test Method for Tensile Properties of Thin Plastic Sheeting*), which are often referred to as uniaxial tension tests, are merely index tests and are discussed only briefly. Rather, the current paper focuses on the measured response of common polymeric geomembranes using established performance tests, such as ASTM D 5617 and D 4885. As neither of these geosynthetic tension tests exactly replicates field conditions, a comparison of the results obtained by both test devices with an evaluation of their respective stress and strain fields would be useful to design engineers. This is the objective of the current paper.

2 BACKGROUND

2.1 General

The multi-axial and wide strip tension test devices, procedures, and interpretations have both been standardized through ASTM, and detailed descriptions of these tests are contained in the ASTM standards referenced in Section 1. Hence, comprehensive discussions of each of these tests are not repeated in the current paper. However, a number of recent studies have clarified some key aspects of these tests, so discussions of these advancements are presented in this section, along with a discussion of previous and ongoing comparisons of wide strip and multi-axial tension test results.

2.2 Wide Strip Uniaxial Tension Testing

The wide strip tension test (ASTM D 4885) was recently re-investigated by Merry and Bray (1996), and the results of their study indicate that, contrary to a common misconception, that this test captures a geosynthetic's response under plane-strain conditions, the wide strip tension test should be considered a uniaxial stress tension test. The wide strip test boundary conditions vary from a plane-strain, biaxial stress state at the clamped ends of the test specimen (i.e. no lateral strains are permitted and the out-of-plane principal stress is essentially zero) to a uniaxial stress state in the middle of the test specimen (i.e. lateral and transverse deformations are not restrained and the lateral and transverse principal stresses are both zero). However, test results presented by Merry and Bray (1996) showed that there is no systematic variation in the stress-strain response of high density polyethylene (HDPE) and polyvinyl chloride (PVC) geomembranes due to specimen width to length aspect ratio variations over a range of 0.1 to 5.5. Over this range of aspect ratios, which included values as low as those used in the "index" uniaxial tension tests (i.e. aspect ratio of 0.1 to 0.2 for ASTM D 882 and D 638) and values almost three times that specified in the wide strip tension test (i.e. an aspect ratio of 2.0 for ASTM D 4885), the nearly pure uniaxial stress field within the test specimen away from the clamps governs the membrane's overall stress-strain response. Thus, the wide strip tension test should be considered a uniaxial stress state performance test, not a plane-strain test, and in the remainder of the current paper, it will be referred to as the uniaxial tension test.

The ASTM D 638 and D 882 test methods for evaluating the tensile characteristics of plastics are commonly considered uniaxial tension tests, albeit index tests. Giroud et al. (1994) evaluated the distribution of strains within the dumbbell specimen used in the ASTM D 882 uniaxial tension test, and they recommended that strain be calculated across the specimen's central section using an extensometer as opposed to using gage separation. In addition, conventional procedures for these types of tests evaluate stress based on the original area of the specimen (i.e. nominal stress as opposed to true stress), and this overestimates the cross-sectional area during the test, especially after cold draw (necking) initiates. As such, these tests cannot be relied upon to accurately characterize the stress-strain response of geomembranes. However, using ASTM D 882 size specimens, Merry and Bray (1996) found that reasonable performance data can be obtained from these tests if the specimen's extension is measured accurately across a uniform specimen width and if true stress is calculated using the actual area during testing. Hence, if properly executed and interpreted, these index tests can provide useful insight regarding the uniaxial response of geomembranes.

2.3 Multi-Axial Tension Testing

The multi-axial tension test ideally provides boundary conditions that vary from a plane-strain, biaxial stress state at the restraining clamps (i.e. no lateral strains are permitted and the out-of-plane principal stress is essentially zero) to a nearly isotropic biaxial stress state at the center (i.e. deformations are not restrained and balanced in-plane membrane stresses exist with the out-of-plane stress equal to zero on the outside of the membrane). The out-of-plane stress acting on the inside of the membrane is actually nonzero and equal to the applied internal air pressure. However, this pressure is resisted by the in-plane tensile stresses due to the curved deflected shape of the membrane. Hence, the overall out-of-plane stress effect on the membrane is considered to be minor, so that a nearly isotropic biaxial stress state is achieved at the center of the membrane.

Several apparatuses and interpretations for multi-axial tension testing of membranes have been developed (e.g. Treloar 1944; Adkins and Rivlin 1952; Steffen 1984; Giroud et al. 1990; Koerner et al. 1990; Caldwallader 1991; Frobel and Taylor 1991; Duvall 1993; Nobert 1993; Merry et al. 1993; and Merry and Bray 1997a). These studies have provided useful insight regarding this relatively new test for evaluating the stress-strain response of geomembranes, and many of these insights have been incorporated into the ASTM D 5617 standard test procedure for the multi-axial tension test. Moreover, rapid development in this field has led to design procedures based on the multi-axial test (e.g. Giroud et al. 1990; Koerner and Hwu 1991; Berg and Collin 1993; Merry et al. 1995). However, a number of key multi-axial test and interpretation issues are not widely accepted, and these key issues require discussion.

Currently, ASTM D 5617 requires a minimum diameter clamping ring of 450 mm, but theoretical and experimental results allow the use of smaller clamping rings as long as the ratio of the ring's diameter to the thickness of the material tested is at least 60 (Merry and Bray 1995). In addition, the D 5617 recommended pressure-controlled loading produces uncontrollable and variable strain rates, particularly in the vicinity of failure. Instead, multi-axial testing should be performed with a strain-controlled loading algorithm that allows for unambiguous interpretation of the strain-rate dependent, stress-strain response of most geomembranes. Moreover, this type of loading allows for direct comparison of the results with those obtained from uniaxial tension testing, which also uses strain-controlled loading. Likewise, where evaluation of a geomembrane's creep response is desired, constant membrane stress (not constant internal test pressure) creep tests are preferred (Merry and Bray 1997a). Lastly, the average stress induced in the geomembrane at various center-point deflections should be calculated using the true stress equation developed by Merry et al. (1993) in lieu of the nominal stress formula contained in D 5617, as it is based on a constant geomembrane-volume (incompressible) hypothesis, which is the expected response of most polymeric geomembranes (Koerner 1998).

Whereas testing and analysis has shown that even the wide strip tension test is effectively a uniaxial stress tension test (Merry and Bray 1996), the stress and strain field governing the multi-axial tension test is less clear. A well-executed wide strip test produces "failure" in the test specimen's midsection, where a uniaxial stress state exists, and a test specimen's overall response has been found to be governed (and can be interpreted) by this uniaxial stress state. A well-executed, multi-axial tension test also produces "failure" in the middle of the test specimen: where a nearly isotropic biaxial stress state exists. Thus, one might suspect that the overall response of the multi-axial, tension test specimen is governed by the nearly isotropic biaxial stress state in its middle. However, experimental evidence to collaborate this suspicion is lacking, due to the unavailability of purely plane-strain, membrane testing and the difficulty of defining the transition from the plane-strain, biaxial stress state near the restraining ring to the isotropic biaxial stress state at the center of the multi-axial test specimen where longitudinal and transverse deformations are permitted. The proximity of the boundary in the multi-axial test suggests that the test specimen is more influenced by boundary conditions in the multi-axial test device in comparison with the uniaxial test device. An experimental investigation of the strain distribution across a membrane in a multi-axial device is discussed in Section 4.

2.4 Relationship Between Uniaxial and Multi-Axial Testing

Few studies have investigated the relationship between uniaxial and multi-axial tension testing of geosynthetics. Studies such as those published by Giroud et al. (1994) and Merry and Bray (1996) have provided useful insights regarding uniaxial tension testing, and studies such as those published by Giroud et al. (1990), Duvall (1993), and Merry and Bray (1995) have provided useful insights regarding multi-axial tension testing. Yet, direct comparisons of the test results from these dissimilar testing devices are lacking. As discussed, the uniaxial tension test provides boundary conditions that vary from a plane-strain, biaxial stress state at the clamps to a uniaxial stress state in the middle, and the multi-axial tension test provides boundary conditions that vary from a plane-strain, biaxial stress state at the restraining clamps to a nearly isotropic biaxial stress state at the center. Thus, it is interesting to investigate how the stress-strain response of geosynthetics are affected by these different test boundary conditions.

Soderman and Giroud (1995), updating the relationships originally derived by Giroud (1992), present theoretical relationships between biaxial and uniaxial tensile characteristics (i.e. secant Young's modulus, yield stress, and yield strain) based on assumptions that the geosynthetic is an isotropic linear elastic material and that the material yields at a given distortion strain energy regardless of the state of stress according to the Mises yield criterion. Secant Young's modulus is defined between the origin and yield point in the stress-strain diagram. At the yield point, Soderman and Giroud (1995) show that the ratio of secant Young's modulus for a material undergoing an isotropic biaxial stress state, E_{ib}, to that for the same material undergoing a uniaxial stress state, E_u, is:

$$\frac{E_{ib}}{E_u} = \frac{1}{1 - \nu} \tag{1}$$

where ν is the engineering Poisson's ratio.

For an incompressible material at less than 10% strain, Poisson's ratio is very close to 0.5. Thus, the theoretical ratio of secant Young's modulus for an isotropic biaxial stress state to that for a uniaxial stress state would be 2.0. This factor is a result of both stress states having identical yield stresses, but the yield strain for the isotropic biaxial stress state being only half of the yield strain for the uniaxial stress state (Soderman and Giroud 1995). Similarly, a theoretical value of 1.33 for an incompressible material was developed for the ratio of the secant modulus between the plane-strain, biaxial stress state and the uniaxial stress state, due to the plane-strain, biaxial stress state having a slightly higher yield stress (1.15 times higher) and slightly lower yield strain (0.87 times lower) than those values in the uniaxial stress state (Soderman and Giroud 1995). As pointed out by Giroud et al. (1993), while these theoretical relationships are potentially useful to design engineers, there is a need to evaluate these theoretical findings against laboratory tests, because the stress-strain-time response of most geomembranes has been shown to be clearly visco-elastoplastic, not linear elastic, and due to the machining process, slightly anisotropic, rather than isotropic (e.g. Merry and Bray 1997a).

3 TESTING PROGRAM

A program of laboratory testing of similar materials was performed to investigate the relationship between uniaxial and multi-axial tension testing. Uniaxial tension testing is performed following the ASTM standard test procedure for the wide strip tension test (D 4885) using the uniaxial tension test apparatus described in Merry and Bray (1996) and shown in Figure 1. Multi-axial tension testing was performed following the ASTM standard test procedure for this test (D 5617), with the modifications recommended by Merry and Bray (1995) discussed in Section 2.3, using the strain-controlled multi-axial tension test device developed by Merry and Bray (1995) and shown in Figure 2. All testing was conducted in a temperature-controlled room at a temperature of $21 \pm 1^\circ$C. Data acquisition was performed with ATS software for Windows (Sousa and Chan 1991) at a high rate of acquisition and accuracy (Merry and Bray 1995, 1996).

At strain levels appropriate for design, there is essentially no difference between engineering strain and true/natural strain, but there can be significant differences between the nominal stress calculated using the original area and true stress calculated using the actual area (Merry and Bray 1996). Hence, for both multi-axial and uniaxial tests results, graphs of average membrane true stress versus engineering strain are presented, which are generated using the equations given below. These equations are based on the assumption that the geomembrane deforms as an incompressible material. For the uniaxial tension test, the stress and strain formulas are (Merry and Bray 1996):

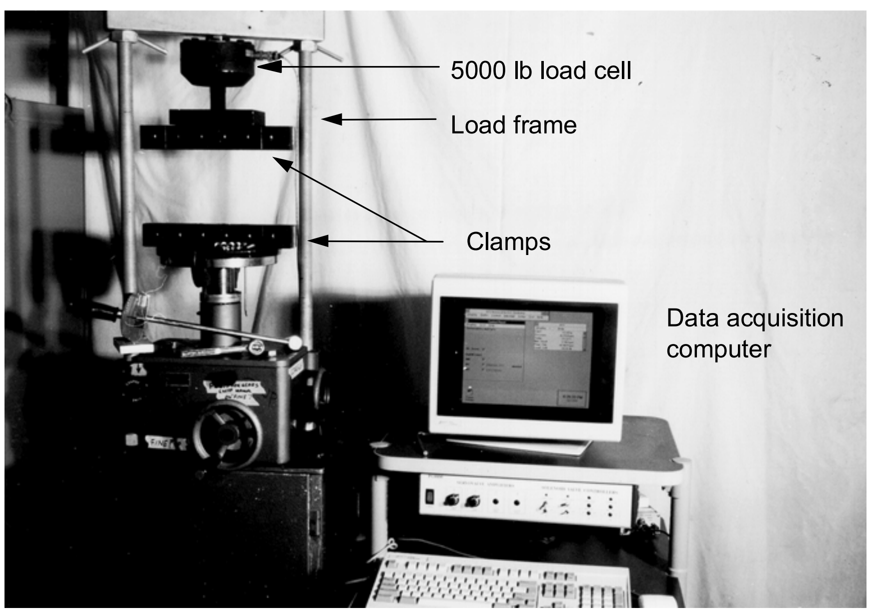

Figure 1. Uniaxial tension testing and data acquisition system (from Merry and Bray 1996).

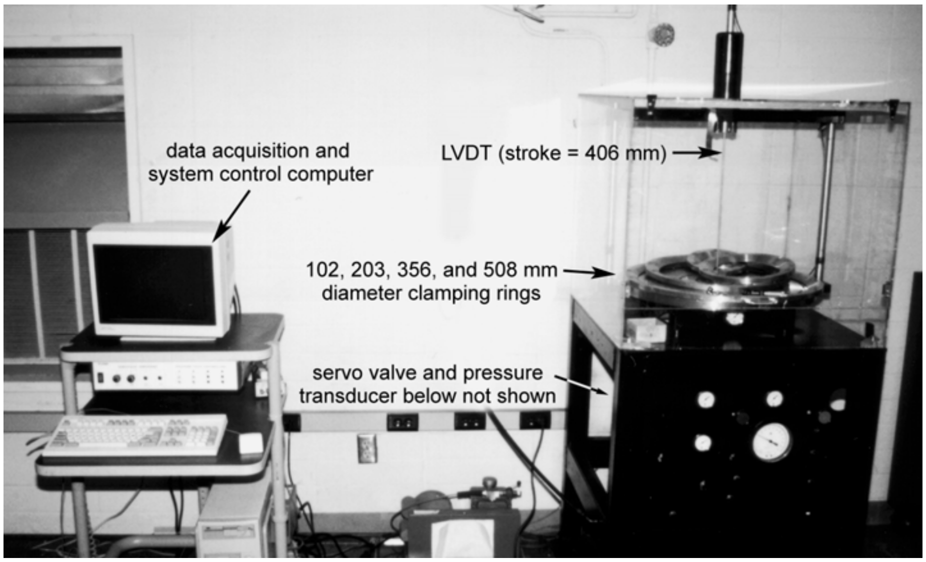

Figure 2. Multi-axial tension testing and data acquisition system (from Merry and Bray 1997a).

$$\sigma_u = \frac{F}{t\,w\,(1 - \nu\,\varepsilon_a)^2} \tag{2}$$

$$\varepsilon_a = \frac{\Delta L}{L_o} \tag{3}$$

$$\nu = \frac{\sqrt{1 + \varepsilon_a} - 1}{\varepsilon_a \sqrt{1 + \varepsilon_a}} \tag{4}$$

where: σ_u = average true membrane uniaxial stress; ε_a = axial engineering strain; F = measured tensile force; L_o = original (untensioned) length of the geomembrane between the grips; t = original geomembrane thickness; w = original geomembrane width; and ΔL = overall geomembrane elongation. For the multi-axial tension test, the equation for the average true membrane stress is (Merry et al. 1993):

$$\sigma = \frac{(L^2 + 4\,\delta^2)^2\,p}{16\,\delta\,L^2\,t} \quad \text{for all } \delta \text{ and constant geomembrane volume} \tag{5}$$

where: p = internal pressure during testing; L = original (untensioned) diameter of the geomembrane (or diameter of the apparatus over which the geomembrane is clamped); and δ = deflection at the center of the geomembrane during the test.

Giroud et al. (1990) and Koerner et al. (1990) presented Equation 6 for calculation of the strain when $\delta < L/2$, and Giroud et al. (1990) and Merry et al. (1993) presented Equation 7 for calculation of the strain when $\delta \geq L/2$:

$$\varepsilon = \left[\frac{\tan^{-1}\left(\frac{4 L \delta}{L^2 - 4\delta^2}\right)\left(\frac{L^2 + 4\delta^2}{4\delta}\right) - L}{L} \right] \quad \text{for} \quad \delta < L/2 \tag{6}$$

$$\varepsilon = \left[\frac{\left(\frac{L^2 + 4\delta^2}{4\delta}\right)\left(\pi - \sin^{-1}\left(\frac{4 L \delta}{L^2 + 4\delta^2}\right)\right) - L}{L} \right] \quad \text{for} \quad \delta \geq L/2 \tag{7}$$

where ε is the engineering strain.

To minimize the material contribution to differences between the tests, initially a series of multi-axial and uniaxial tests were performed on specimens of a nearly isotropic, linear-elastic membrane. The membrane used was a l.65 mm thick latex membrane. All of these tests were performed at a strain rate of approximately 7% per minute. The elastic latex membrane was loaded to approximately 50% strain and then fully unloaded. Subsequently, uniaxial and multi-axial tension tests were performed on two polymeric geomembranes: (i) 0.75 mm (30 mil) thick PVC geomembrane; and (ii) 1.5 mm (60 mil) thick HDPE geomembrane. These tests were performed at the standard strain rate of 1% per minute. Uniaxial tension tests were performed using ASTM D 4888 size specimens (i.e. 200 mm wide by 100 mm long), except the latex specimens were slightly larger. Multi-axial tension tests were performed typically using a 203 mm diameter clamping ring, but some tests were conducted using 102 and 508 mm diameter rings, and no systematic difference in results was observed. The resulting stress-strain data are not smoothed.

4 STRAIN DISTRIBUTION IN MULTI-AXIAL TEST SPECIMEN

Strain fields within the multi-axial device can be examined through observations and geometrical considerations. External measurements of the test specimen's deformed shape and measurement of the volume of water intruded during multi-axial testing using a range of clamping ring diameters indicate that the multi-axial test specimen deforms as a portion of a sphere (Merry and Bray 1995). Using common geometrical formulations for a sphere and a circle (Moffit and Bouchard 1975) and assuming that the membrane longitudinal strain across the test specimen undergoing multi-axial testing is uniform (which appears reasonable based on photographs by Frobel and Taylor (1991) of deformed membranes with grids), the longitudinal strain can be compared to the transverse strain within the membrane along the circumference of a circle centered about the pole of the sphere. At the pole, as pointed out by Duvall (1993), the longitudinal strains in two perpendicular directions are equal and, hence, the specimen is in a nearly isotropic biaxial stress state. However, at a quarter of the radius from the pole (a distance that encompasses only 6.25% of the total test specimen area), theoretically, the transverse strain is approximately 94% of the longitudinal strain. At half of the radius from the pole (includes 25% of the total specimen area), the transverse strain is 75% of the longitudinal strain, and at three-quarters of the radius from the pole (includes 56% of the total specimen area), the transverse strain is only 44% of the longitudinal strain. Of course, at the clamped edge, the transverse strain is zero and the specimen is in a plane-strain, biaxial stress state. Hence, a majority of the multi-axial test specimen is not in an isotropic biaxial stress state, and the test boundary conditions impose a strain field that is intermediate to an isotropic, biaxial stress state and a plane-strain, biaxial stress state.

To investigate the strain distribution in a multi-axial test specimen, a nearly elastic latex membrane was subdivided into segments as shown in Figure 3. Each segment on the membrane was measured carefully using a pair of digital calipers. Photographic methods were not used, because the effects of parallax would be large along a spherical surface, and strain gages were considered to be too stiff relative to the membrane, thus affecting local measurements. Air pressure was increased to deform the latex mem-

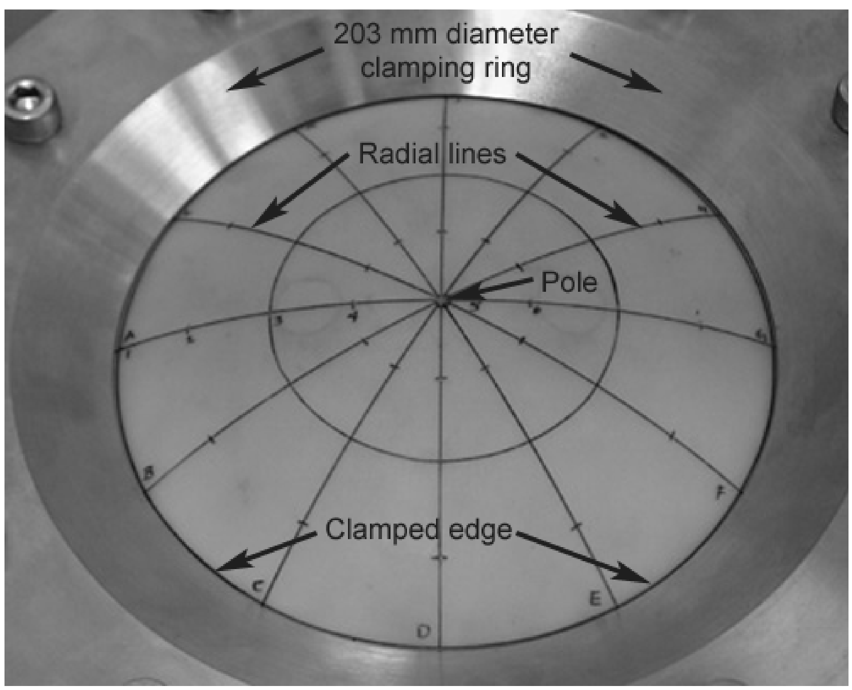

Figure 3. Markings for making strain measurements on test specimen in the multi-axial device (picture taken at a total longitudinal strain of approximately 5%).

brane to the proper centerline deflection. The deformed shape of the latex remained essentially constant during measurements because the latex does not creep.

The measured values from one point to another point along the radial lines represent the longitudinal chord lengths along an assumed sphere. The arc lengths were then calculated using standard geometrical equations (Moffit and Bouchard 1975). The repeatability of longitudinal strain measurements varied by approximately 1%, due to the limitations of measuring small changes in segment lengths as the membrane deformed over a strain range of 1 to 5%. While the measured values of total longitudinal strain across the entire membrane were in good agreement with the value calculated using Equation 6 (within a fraction of a percent; a similar finding to studies presented in Merry 1995), the distribution of segmental longitudinal strains varied somewhat across the membrane. Systematic variations could not be discerned because of the scatter in the data.

Transverse strain measurements represented by the strain between two points on adjacent radial lines were also taken. Measurements at larger strain values were made to minimize scatter. Figure 4 shows the variation in the measured transverse strain at a total longitudinal strain of 20.6%. The repeatability of transverse strain measurements varied from a percent to a few percent. The scatter increases as the pole is approached because the distance between adjacent radial lines is shorter near the pole and, hence, the error made in the measurements is a larger percentage of the measured value. The measured transverse strain at a quarter of the ring diameter from the pole was slightly less than the total longitudinal strain across the membrane, as suggested by theory. Additionally, the measured transverse strain was consistent with the theoretical values of 75 and 44% of the total longitudinal strain at the half radius and three-quarters location from the pole, respectively. Thus, these measurements confirm the theoretical trends described previously, indicating that the transverse strain transitions in a predictable manner from 100% of the longitudinal strain at the pole to 0% of the longitudinal strain at the clamped edge.

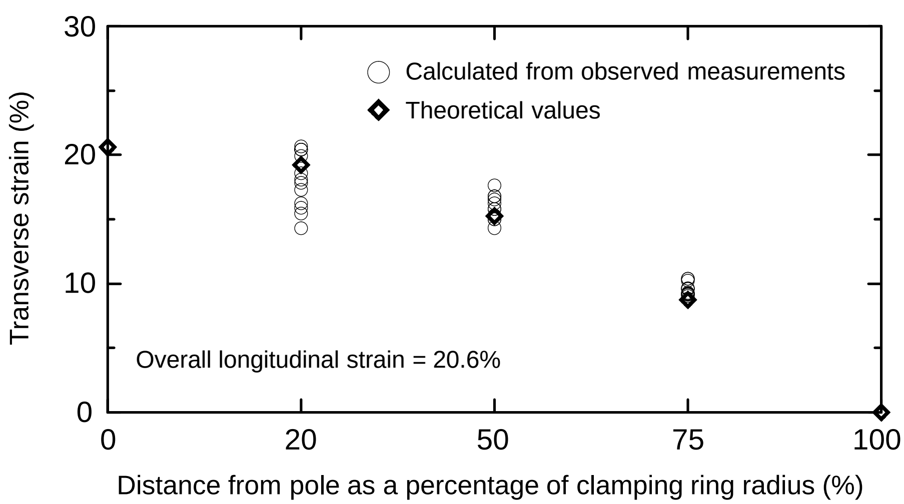

Figure 4. Variation of transverse strain as a function of distance from the pole at a total longitudinal strain of 20%.

Although the significant scatter in these measurements preclude developing detailed findings regarding the variations of strain across a membrane in a multi-axial test device, these measurements confirm that longitudinal strains across the deformed membrane are relatively uniform and that the total longitudinal strain can be reliably estimated with Equation 6. However, significant relative variations in strain across a membrane can occur at low strains in the multi-axial device. In addition, a nearly isotropic biaxial stress state with nearly equal longitudinal and transverse strains occurs within the middle of the specimen, such that the multi-axial test device can be considered to replicate a nearly isotropic biaxial stress state with fairly uniform strains in this region; but, near the clamped edges, the multi-axial test does not represent an isotropic biaxial stress state.

5 UNIAXIAL AND MULTI-AXIAL RESULTS AND DISCUSSION

5.1 Elastic Latex Membrane

Five multi-axial tension tests and four uniaxial tension tests were performed using the 1.65 mm thick latex membrane. The results presented in Figure 5 show the average true stress versus strain from these tests (multi-axial stresses calculated per Equation 5). These results indicate that this material is nearly linear elastic, particularly considering that the induced maximum strain of 50% is more than twice the strain range of interest for geomembranes (i.e. considerably lower than 20%). Figure 6 shows the results

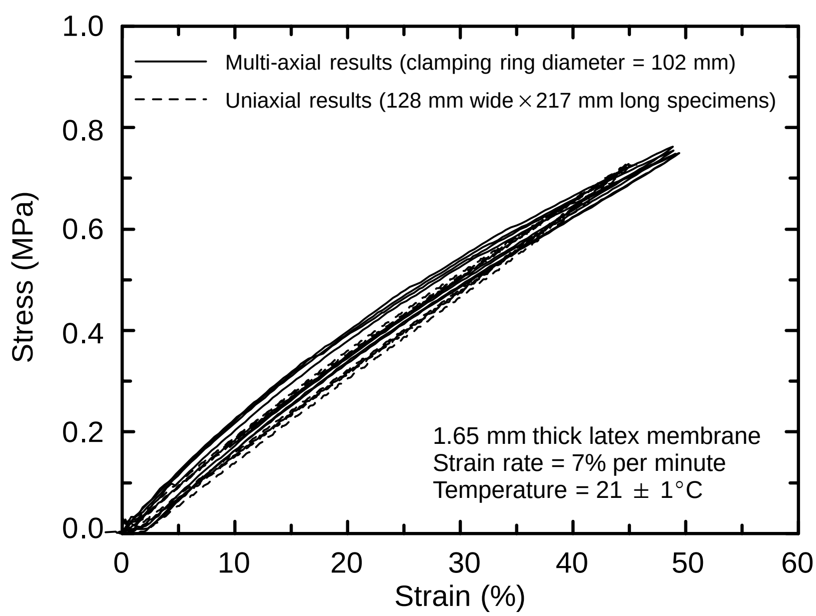

Figure 5. Multi-axial and uniaxial tension test results for a 1.65 mm thick latex membrane showing full load-unload response.

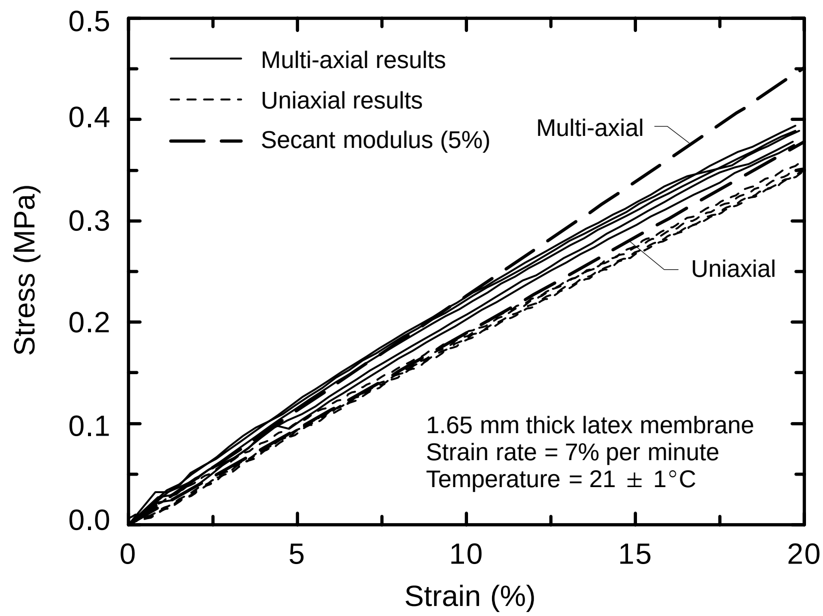

Figure 6. Multi-axial and uniaxial tension test results from Figure 5 showing initial primary loading only.

of these tests for primary loading only over a reasonable strain range of interest (less than 20%). The ratio of the multi-axial to uniaxial secant Young's modulus (defined from the origin to a specified point on the stress-strain curve) over this strain range varies from 1.1 to 1.3. The secant modulus at 5% strain for both test conditions is also shown in Figure 6 and, at this level of strain, the ratio of the secant modulus is approximately 1.2.

During multi-axial testing, the stress conditions at the center of the test specimen most closely represent an isotropic, biaxial stress condition. Based on the methodology of Giroud et al. (1990) for calculating geomembrane tension with a constant thickness material, Duvall (1993) presented equations for calculating the true, isotropic biaxial stress and strain for an incompressible material. Merry (1995) showed that for $\delta < L/2$, the equation provided by Giroud et al. (1990) for calculating the strain during the multi-axial test is identical to Equation 6 and that the equations for calculating the isotropic biaxial stress at the pole given by Duvall (1993) simplify to:

$$\sigma = \frac{(L^2 + 4\,\delta^2)\,(1 + \varepsilon)^2 p}{16\,\delta\, t} \quad \text{for} \quad \delta < L/2 \tag{8}$$

with ε given by Equation 6. The consequence of calculating the stresses with Equation 5 or 8 is shown in Figure 7 where data from a multi-axial tension test on 1.0 mm thick HDPE has been interpreted with both of these equations. At significant levels of strain (i.e. greater than 5%), the balanced biaxial stresses calculated from Equation 8 are greater than the average true stress as given by Equation 5. However, at strain levels less than 5%, the differences are negligible. As shown in Figure 4, only a limited area

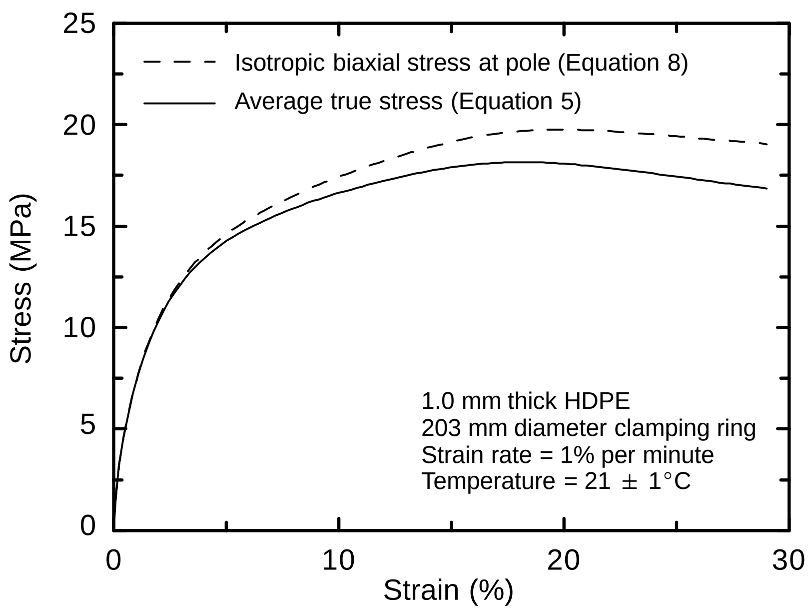

Figure 7. Consequences of calculating average true membrane stress (Equation 5) versus balanced biaxial stress at pole (Equation 8).

of the multi-axial test specimen is in a nearly isotropic, biaxial stress state, so Equation 5 is preferred because using Equation 8 can result in high (unconservative) estimates of the induced membrane stress at larger strain levels. However, to allow a direct comparison with the theoretical study by Soderman and Giroud (1995), Equation 8 was used as a best estimate of the isotropic, biaxial stress state at the pole of the membrane.

Figure 8 shows the elastic membrane test results where the isotropic biaxial stresses at the pole from the multi-axial test have now been calculated using Equation 8. The secant modulus ratio between the isotropic biaxial stress state and uniaxial stress state over the strain range of interest (2 to 20%) ranges from 1.2 to 1.3. Also shown in Figure 8 is the theoretically derived secant modulus at 5% strain for the multi-axial tension test based on the uniaxial tension test results on the nearly linear, elastic latex membrane and the theoretical relationship between isotropic biaxial and uniaxial stress states for an isotropic, linear elastic material developed by Soderman and Giroud (1995). The measured ratio of the isotropic, biaxial secant modulus at 5% strain to that for the uniaxial stress state of approximately 1.2 is significantly less than the theoretical value of 2.0. This discrepancy could arise from a limitation resulting from the simplifying assumptions required in the theoretical derivation or from the limitation of the multi-axial test device to produce a perfectly isotropic, biaxial stress state at the center of the test specimen. Nevertheless, until this discrepancy between theoretical and experimental results can be resolved, it is recommended to place greater weight on the consistent laboratory test results. Hence, for an isotropic, linear elastic material, the ratio of the secant modulus for the isotropic, biaxial stress state to that measured in the laboratory using the uniaxial tension test is most likely within the range of 1.2 to 1.3, and based on this bound,

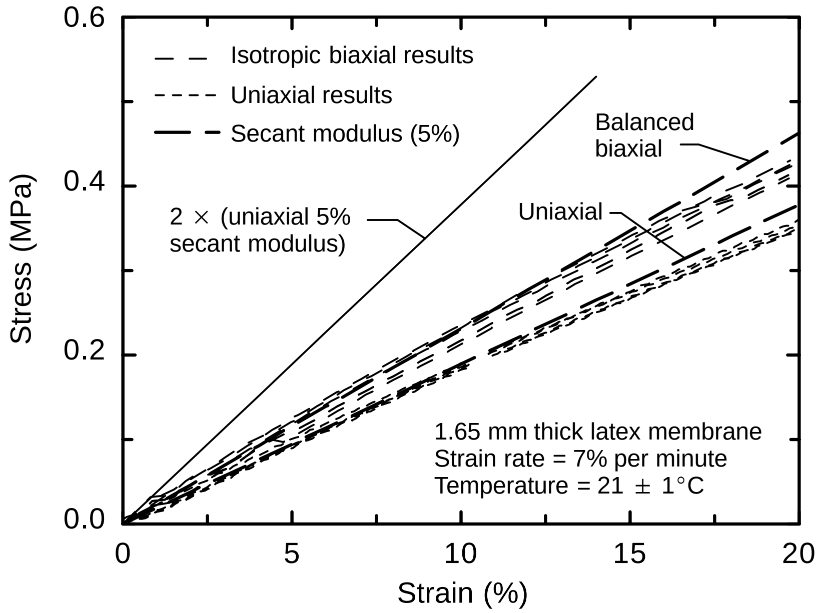

Figure 8. Balanced biaxial and uniaxial tension test results for elastic membrane using biaxial stress calculation at pole (Equation 8).

the ratio of the secant modulus for a plane-strain, biaxial stress state to that from the uniaxial test is within the range of 1.0 to 1.3 (i.e. this ratio should be between the measured multi-axial to uniaxial secant modulus ratio and one).

5.2 PVC Geomembrane

Six multi-axial and five uniaxial tension tests were performed on the 0.75 mm thick PVC geomembrane. The results are presented in Figure 9. Again, the individual test results are fairly consistent for this manufactured material, with the multi-axial tension test results exhibiting a stiffer response than the uniaxial test over the strain range of interest (i.e. less than 20%). The stress-strain response of the PVC geomembrane is only slightly nonlinear over the strain range of interest, and one might expect the comparison the multi-axial and uniaxial PVC test results to be similar to that presented for the linear elastic latex membrane. Individual test results were averaged by calculating the induced average stress at each strain level, and these average multi-axial and uniaxial test results are shown in Figure 10. For these test conditions, the observed ratio of the multi-axial to uniaxial secant modulus remained almost constant over a range of 2 to 10% strain (i.e. 1.50 to 1.40, with an average of 1.43). At 6% strain, the observed ratio is 23.4 MPa/16.6 MPa, or approximately 1.4. Correspondingly, the strength (i.e. mobilized stress at a specified strain) is slightly less for the uniaxial test compared to the multi-axial test, and the material's failure strain (i.e. strain at the maximum stress) was not reached in these tests, which were terminated at a strain of approximately 100%.

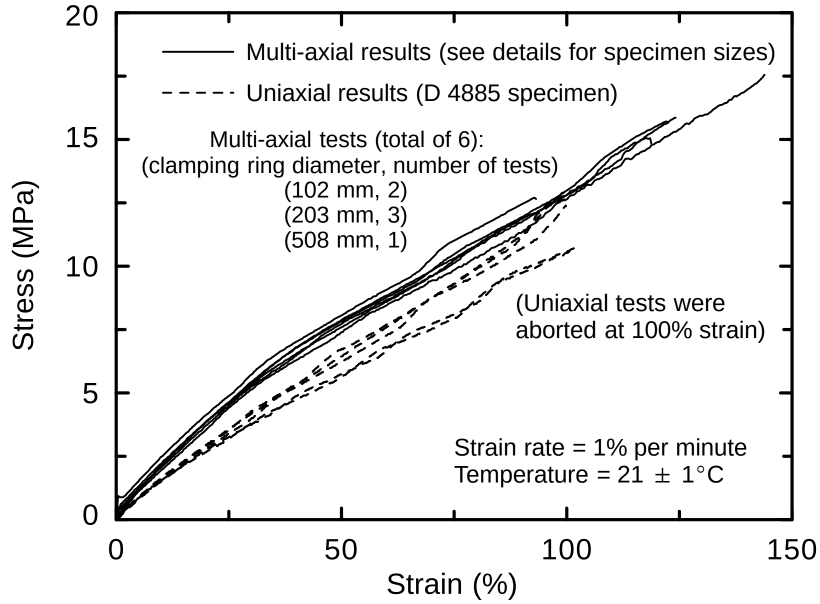

Figure 9. Multi-axial and uniaxial tension test results for 0.75 mm thick PVC geomembrane.

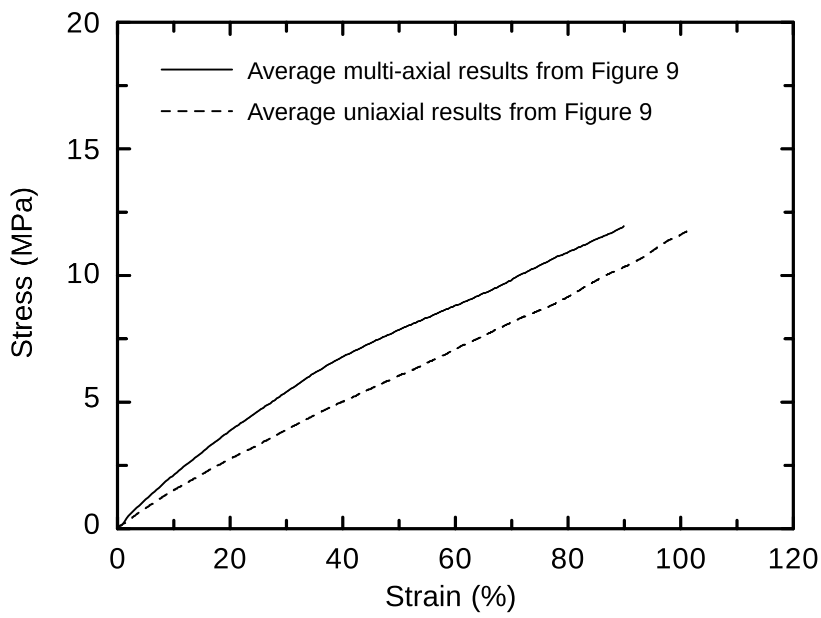

Figure 10. Comparison of average multi-axial and uniaxial tension test results for PVC specimens.

5.3 HDPE Geomembrane

Six multi-axial and four uniaxial tension tests were performed on the 1.5 mm thick HDPE geomembrane. The results are presented in Figure 11. The individual HDPE test results are even more consistent than the PVC test results discussed in Section 5.2, and again, the multi-axial results exhibit a stiffer response initially than the uniaxial results. However, comparing Figure 11 with Figure 9, it is clear that the stress-strain response of the HDPE geomembrane is highly nonlinear compared to that of the PVC geomembrane. Average results for HDPE for both test conditions are shown in Figure 12. Due to the nonlinearity, the observed ratio of multi-axial to uniaxial secant modulus is dependent on the strain level and decreases as the strain increases. At 0.5% strain, the ratio is 922 MPa/383 MPa or approximately 2.4, at 1% strain, the ratio is 732 MPa/384 MPa or approximately 1.9, and at 2.0% strain, the ratio is 528 MPa/364 MPa or approximately 1.45. At 5% strain, this ratio is approximately 1.1 and, effectively, 1.0 at strains greater than 10%. Both tests indicate the maximum induced membrane stress (i.e. strength) of the HDPE geomembrane is approximately 18.7 MPa. As a point of reference, the manufacturer of this HDPE geomembrane measured a yield stress and yield strain of 17.5 MPa and 16.3%, respectively, using the ASTM D 638 "index" uniaxial tension test and conventional procedures (i.e. nominal stress instead of true stress).

Besides the initially stiffer response of the HDPE geomembrane in the multi-axial tension device (an observation consistent for all materials tested in the current study), the HDPE uniaxial and multi-axial test results differ in one more important aspect. The average HDPE multi-axial test results show a peak induced membrane stress of approx-

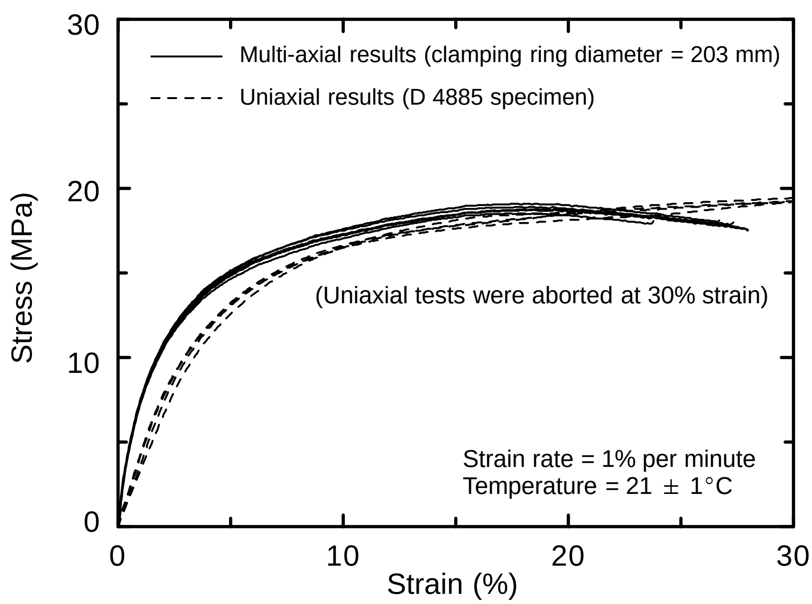

Figure 11. Multi-axial and uniaxial tension test results for 1.5 mm thick HDPE geomembrane.

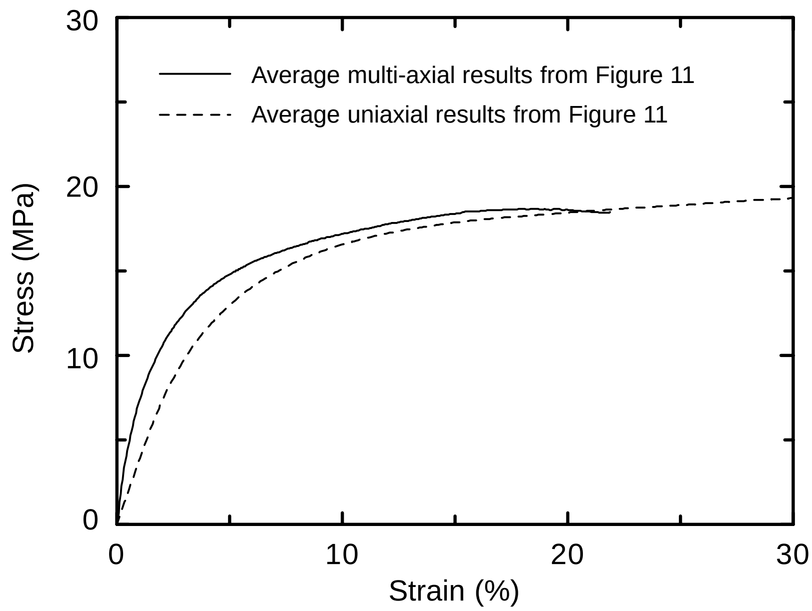

Figure 12. Comparison of average multi-axial and uniaxial tension test results for HDPE specimens.

imately 18.7 MPa at a strain of approximately 19.5%. However, for the same material, the average HDPE uniaxial test results show a continuous increase in the calculated induced membrane stress over the entire duration of the test (uniaxial tests were aborted at 30% strain). The determination of failure strain (strain at maximum membrane stress) for a mildly strain-softening material such as HDPE is not possible using the uniaxial tension test when the test results are plotted as true stress versus strain. If the data is plotted as nominal stress versus strain, a peak stress and corresponding failure strain is sometimes observed, but this peak nominal stress is fictitious and, hence, the corresponding failure strain is also fictitious.

Thus, the uniaxial tension test (when properly interpreted) could lead to unconservative estimates of the ductility of a geomembrane; whereas, the multi-axial tension test is able to capture the peaking of induced membrane stress and define the strain at which this occurs (i.e. the material's failure strain). For HDPE materials, the failure strain has repeatedly been found to be within the range of 16 to 20% in the multi-axial device at strain rates of 1% per minute at 21°C (e.g. Merry and Bray 1997a). Failure strain has been shown to be both strain rate (Merry and Bray 1997a) and temperature (Merry and Bray 1997b) dependent, with the failure strain decreasing as the strain rate increases or as the temperature decreases. Definition of a material's failure strain is of paramount importance when using an allowable strain design approach, such as that recommended by Giroud et al. (1993).

6 CONCLUSIONS

Both the multi-axial and wide strip tension tests provide varying boundary conditions for the specimen during testing. The wide strip tension test imposes boundary conditions that vary from a uniaxial stress state near the middle of the specimen to a plane-strain, biaxial stress state at the clamps. The multi-axial tension test imposes boundary conditions that vary from a plane-strain, biaxial stress state at the restraining ring to a nearly isotropic, biaxial stress state at the center. A critical re-examination of the wide strip tension test (ASTM D 4885) has found that the membrane's overall response is governed by its uniaxial stress response away from the clamped ends (Merry and Bray 1996). Therefore, the wide strip tension test is simply a performance-oriented uniaxial tension test. Interpretation of the multi-axial tension test is not unambiguous, but the membrane's response is intermediate between that in a nearly isotropic, biaxial stress state and a plane-strain, biaxial stress state. The longitudinal and transverse strains across the middle of the test specimen (i.e. area within a circle centered at the pole and having a radius of half of the specimen radius) are fairly uniform and essentially balanced. However, the middle of the specimen constitutes only a quarter of the total specimen area, and the remaining part of the test specimen is affected by the plane-strain, biaxial stress state imposed at the clamped edge of the specimen. Hence, it appears reasonable and it is conservative regarding strength and failure strain to interpret the multi-axial tension tests data using Equation 5, which provides the average true membrane stress for the test specimen, rather than Equation 8, which assumes a purely isotropic, biaxial stress state.

The average stress-strain response obtained from the multi-axial tension test was compared with that from the uniaxial tension test and the secant Young's modulus results are summarized in Table 1. The uniaxial response was found to be similar in peak strength, but softer in the initial secant modulus, compared to the multi-axial response. More importantly, determination of the material's failure strain from the uniaxial tension test results may not be possible. For materials that exhibit a mild post-peak strain-softening response, such as HDPE, the multi-axial tension test device offers the superior advantage of being able to capture this response and identify the material's failure strain.

Table 1. Summary of test results comparison.

Material	Secant modulus ratios	
	$\frac{E_{ib}}{E_u}$	$\frac{E_{ps}}{E_u}$
Linear elastic - theoretical (Soderman and Giroud 1995)	2.0	1.33
Elastic latex membrane	∼1.2	1.0 to 1.2
PVC geomembrane	∼1.4	1.0 to 1.4
HDPE geomembrane	∼1.9*	1.0 to 1.9*

Note: * At ε = 1% strain.

The trends in the multi-axial and uniaxial tension test results (i.e. higher secant modulus for multi-axial results compared to uniaxial results) were found to be consistent for all three materials tested (i.e. elastic latex, PVC, and HDPE geomembranes). However, the magnitude of the ratio between the secant modulus for a balanced, biaxial stress state obtained from the multi-axial tests to those from the uniaxial tests varied with test material. Experimental results from the isotropic "linear" elastic latex membrane showed this ratio was within the range of 1.1 to 1.3, which is significantly less than the theoretical ratio of 2.0 as presented by Soderman and Giroud (1995). In fact, the measured secant modulus ratio is closer to that derived for the modulus ratio of plane-strain, stress state to uniaxial stress state (theoretically, a value of 1.33). Based on test results for two common geomembrane materials, PVC and HDPE, the multi-axial to uniaxial secant modulus ratio was approximately 1.4 (at 2 to 10% strain) for the PVC geomembrane, and at the commonly used 1% strain level, the secant modulus ratio was 1.9 for the HDPE geomembrane, but the secant modulus ratio varied significantly with strain level for the HDPE geomembrane. These results were obtained at strain rates of 1% per minute at a temperature of 21°C and, due to the visco-elastoplastic nature of these polymeric geomembranes, these values would need to be adjusted for other test conditions. The stress-strain data presented for these materials (e.g. Figures 6, 9, and 11) indicate that the latex membrane response is nearly linear elastic, the PVC geomembrane response is only slightly nonlinear, and the HDPE geomembrane response is highly nonlinear. Correspondingly, the multi-axial to uniaxial secant modulus ratio at strain levels commonly used in practice increases from approximately 1.2 for the latex membrane, to approximately 1.4 for the PVC geomembrane, and to approximately 1.9 for the HDPE geomembrane. Hence, the difference between the multi-axial and uniaxial tension test results is more significant for materials exhibiting more nonlinearity in their stress-strain response, especially at low strain levels where the secant modulus is a more sensitive parameter.

Considering the findings of the current study and the stress and strain fields common in a number of field applications of geosynthetics (e.g. plane-strain, biaxial stress dragdown of side slope liners in waste fills; plane-strain, biaxial stress deformation of continuous reinforcing layers in mechanically stabilized earth; and isotropic, biaxial stress subsidence of a geomembrane overlying a void), the multi-axial tension test device offers superior boundary conditions and will often be the most appropriate performance test for geosynthetics. Moreover, the multi-axial tension test offers the significant advantage of capturing the ductility (i.e. failure strain) of a geomembrane's response. As the ASTM D 5617 minimum clamping ring diameter of 450 mm has been shown to be unnecessary (Merry and Bray 1995), good performance-oriented test results can be obtained from 100 to 200 mm diameter tests conducted on specimens available from the 305 mm width commonly removed from every other roll of manufactured geomembranes for quality control testing. Hence, wider use of the multi-axial test device is recommended.

However, for cases in which the geosynthetic will deform in principally a uniaxial stress state (e.g. isolated geosynthetic reinforcing strips) or when only checking the peak strength of the geosynthetic, the wide strip uniaxial tension test is appropriate. For cases in which uniaxial test results are available and a material's multi-axial response requires assessment, the engineer should assume that the material's multi-axial stress-strain response will be initially stiffer (e.g. for this study, approximately 1.4 times stiffer for PVC) and significantly less ductile (e.g. for this study, multi-axial HDPE failure strains on the order of 16 to 20%).

ACKNOWLEDGEMENTS

Financial support was provided by the David and Lucile Packard Foundation, and the National Science Foundation under Grant BCS-9157083, and this support is gratefully acknowledged. HDPE samples were provided by National Seal, Inc.; PVC samples were provided by Environmental Protection, Inc.; and latex samples were obtained from 3D Polymers, Gardena, California.

REFERENCES

Adkins, J.E. and Rivlin, R.S., 1952, "Large Elastic Deformations of Isotropic Materials IX. The Deformation of Thin Shells", *Philosophical Transactions of the Royal Society of London*, Vol. 244, Series A, pp. 505-531.

ASTM D 638, "*Standard Test Method for Tensile Properties of Plastics*", American Society for Testing and Materials, West Conshohocken, Pennsylvania, USA.

ASTM D 882, "*Standard Test Method for Tensile Properties of Thin Plastic Sheeting*", American Society for Testing and Materials, West Conshohocken, Pennsylvania, USA.

ASTM D 4885, "*Standard Test Method for Determining Performance Strength of Geomembranes by the Wide Strip Tensile Method*", American Society for Testing and Materials, West Conshohocken, Pennsylvania, USA.

ASTM D 5617, "*Standard Test Method for Multi-Axial Tension Test for Geosynthetics*", American Society for Testing and Materials, West Conshohocken, Pennsylvania, USA.

Berg, R.R. and Collin, J.G., 1993, "Design of Landfill Liners Over Yielding Foundations", *Proceedings of Geosynthetics '93*, IFAI, Vol. 3, Vancouver, British Columbia, Canada, March 1993, pp. 1439-1454.

Cadwallader, M.W., 1991, "Addressing the Special Concerns of Landfill Closures: VLDPE and Textured Geomembranes", *Geotextiles and Geomembranes*, Vol. 10, Nos. 5-6, pp. 411-425.

Duvall, D.E., 1993, "Creep and Stress Rupture Testing of a Polyethylene Geomembrane Under Equal Biaxial Stress", *Proceedings of Geosynthetics '93*, IFAI, Vol. 2, Vancouver, British Columbia, Canada, March 1993, pp. 817-830.

Frobel, R.K. and Taylor, R.T., 1991, "CSPE/Geotextile Geocomposites", *Geotextiles and Geomembranes*, Vol. 10, Nos. 5-6, pp. 443-457.

Giroud, J.P., 1992, "Biaxial Tensile State of Stress in Geosynthetics", *Geotextiles and Geomembranes*, Vol. 11, No. 3, pp. 319-325.

Giroud, J.P., Bonaparte, R., Beech, J.F. and Gross, B.A., 1990, "Design of Soil Layer-Geosynthetic Systems Overlying Voids", *Geotextiles and Geomembranes*, Vol. 9, No. 1, pp. 11-50.

Giroud, J.P., Monroe, M. and Charron, R., 1994, "Strain Measurement in HDPE Geomembrane Tensile Tests", *Geotechnical Testing Journal*, Vol. 17, No. 1, pp. 65-71.

Giroud, J.P., Soderman, K.L. and Monroe, M., 1993, "Mechanical Design of Geomembrane Applications", *Proceedings of Geosynthetics '93*, IFAI, Vol. 3, Vancouver, British Columbia, Canada, March 1993, pp. 1455-1468.

Koerner, R.M., 1998, "*Designing With Geosynthetics*", Fourth edition, Prentice Hall, Englewood Cliffs, New Jersey, USA, 761 p.

Koerner, R.M. and Hwu, B-L., 1991, "Stability and Tension Considerations Regarding Cover Soils on Geomembranes Lined Slopes", *Geotextiles and Geomembranes*, Vol. 10, Nos. 5-6, pp. 335-355.

Koerner, R.M., Koerner, G.R. and Hwu, B-L., 1990, "Three Dimensional Axisymmetric Geomembrane Tension Test", *Geosynthetic Testing for Waste Containment Applications*, Koerner, R.M., Editor, ASTM Special Publication 1081, proceedings of a symposium held in Las Vegas, Nevada, USA, January 1990, pp. 170-184.

Merry, S.M., 1995, "*Mechanical Response and Properties of Geomembranes*", Ph.D. Thesis, University of California, Berkeley, California, USA, 486 p.

Merry, S.M. and Bray, J.D., 1995, "Size Effects for Axisymmetric Testing of Geomembranes", *Geotechnical Testing Journal*, Vol. 18, No. 4, pp. 441-449.

Merry, S.M. and Bray, J.D., 1996, "Geomembrane Response in the Wide Strip Tension Test", *Geosynthetics International*, Vol. 3, No. 4, pp. 517-536.

Merry, S.M. and Bray, J.D., 1997a, "Time-Dependent Mechanical Response of HDPE Geomembranes", *Journal of Geotechnical Engineering*, Vol. 123, No, 1, pp. 57-65.

Merry, S.M. and Bray, J.D., 1997b, "Temperature-Dependent Multi-Axial Creep Response of HDPE Geomembranes", *Proceedings of Geosynthetics '97*, IFAI, Vol. 1, Long Beach, California, USA, March 1997, pp. 163-176.

Merry, S.M., Bray, J.D. and Bourdeau, P.L., 1993, "Axisymmetric Tension Testing of Geomembranes", *Geotechnical Testing Journal*, Vol. 16, No. 3, pp. 384-392.

Merry, S.M., Bray, J.D. and Bourdeau, P.L., 1995, "Stress-Strain Compatibility of Geomembranes Subjected to Subsidence", *Proceedings of Geosynthetics '95*, IFAI, Vol. 2, Nashville, Tennessee, USA, February 1995, pp. 799-812.

Moffit, F.H. and Bouchard, H., 1975, "*Surveying*", Sixth edition, Harper & Row, Publishers, New York, New York, USA, 879 p.

Nobert, J., 1993, "The Use of Multi-Axial Burst Test to Assess the Performance of Geomembranes", *Proceedings of Geosynthetics '93*, IFAI, Vol. 2, Vancouver, British Columbia, Canada, March 1993, pp. 685-702.

Soderman, K.L. and Giroud, J.P., 1995, "Relationships Between Uniaxial and Biaxial Stresses and Strains in Geosynthetics", *Geosynthetics International*, Vol. 2, No. 2, pp. 495-504.

Sousa, J. and Chan, C.K., 1991, "Computer Applications in the Geotechnical Laboratories of the University of California, at Berkeley", *Geotechnical Engineering Congress 1991*, McLean, F.G., DeWayne, A. and Campbell, D.W.H., Editors, ASCE Geotechnical Special Publication No. 27, Vol. 1, proceedings of a congress held in Boulder, Colorado, USA, June, pp. 531-543.

Steffen, H., 1984, "Report on Two Dimensional Strain Stress Behavior of Geomembranes With and Without Friction", *Proceedings of the International Conference on Geomembranes*, Denver, Colorado, USA, pp. 181-185.

Treloar, L.R.G., 1944, "Strains in an Inflated Sheet, and the Mechanism of Bursting", *Institution of the Rubber Industry*, Vol. 19, pp. 201-212.

NOTATIONS

Basic SI units are given in parentheses.

F = measured force acting on geomembrane during uniaxial tension test (N)

E = secant Young's modulus (Pa)

E_{ib} = secant Young's modulus for material undergoing an isotropic biaxial stress state (Pa)

E_{ps} = secant Young's modulus for material undergoing a plane-strain, biaxial stress state (Pa)

E_u = secant Young's modulus for material undergoing an isotropic uniaxial stress state (Pa)

L = length of specimen between clamps (m)

L_o = untensioned (original) length of specimen between clamps (m)

p = internal pressure during testing (Pa)

t = original, untensioned thickness of geomembrane specimen (m)

w = original width of geomembrane specimen (m)

ΔL = elongation of test specimen length (m)

δ = deflection at center of geomembrane during multi-axial testing (m)

ε = engineering strain (dimensionless)

ε_a = axial engineering strain with respect to original length (dimensionless)

ε_t = transverse engineering strain with respect to original width or thickness (dimensionless)

ν = engineering Poisson's ratio (dimensionless)

σ_u = average uniaxial tensile stress in middle portion of specimen (Pa)